Numerical Analysis for Two-dimensional Heat Transfer of Superfluid Helium with Phase Transition

Ryo Akasaka[1], Takafumi Noda[2], Kenji Fukuda[3] and Hisayasu Kobayashi[4]

Abstract

The purpose of this paper is to confirm the validity of the numerical model proposed in our previous paper for a two-dimensional analysis. The model can be applied to a wide range of temperatures from superfluid helium to normal fluid helium at vapor state. Two-dimensional numerical analysis for the horizontal channel with the heated bottom was performed, and the results were compared with experimental results. For low heat flux, the temperature profiles at steady state obtained from the analysis showed quantitative agreements with those from the experiment. For higher heat flux, the numerical results were able to represent the experimental temperature profiles qualitatively. In the transient analysis, the model was able to simulate the change of the velocity field caused by the phase transition. It was concluded that the validity of the proposed model in the temperature range including the phase transition was partially verified.

Keywords: Superfluid helium, Normal fluid helium, Phase transition, Numerical analysis, Internal convection

1 Introduction

To discuss the stability of superconducting magnets, a numerical model to represent both the λ-transition and the boiling of helium is needed. However, since there were only a few analytical studies of superfulid helium in tha past, a model applicable to a wide temperature range has not been developed. Gorbounov et al. [1] performed a transient analysis of the

1) Faculty of Humanities, Kyushu Lutheran College, 3-12-16 Kurokami, Kumamoto, 860-8520 Japan, TEL:+81-96-343-1600, FAX:+81-96-343-0354, E-mail: akasaka@klc.ac.jp
2) Mitsubishi Heavy Industries, Ltd. Kobe Shipyard & Machinery Works, 1-1-1 Wadasaki-cho, Hyogo-ku Kobe, 652-8585 Japan
3) Institute of Environmental Systems, Kyushu University, 6-10-1 Hakozaki Higashiku Fukuoka, 812-8581 Japan
4) Atomic Energy Research Institute, Nihon University, 1-8 Kanda Surugadai, Chiyodaku, Tokyo, 101-8308 Japan

superconducting material of 45 T hybrid-magnet. In their analysis, the Navier-Stokes equation was employed as the momentum equation of superfluid helium without any modifications, and no term to represent the thermomechanical effect was introduced. We pointed out that since the thermomechanical effect greatly affects thermal behaviors of helium flow, the, the governing equations should have terms to represent the effect [2], Furthermore, we proposed the new numerical model applicable to a wide temperature range [3]. This model, which is referred to as "the simplified model" hereafter, validity of the model for one-dimensional systems was verified in our previous study [3]. In the present study, the analysis of a two-dimensional system using the proposed model is performed, and the results are compared with those obtained from experiment.

2 Numerical model

2.1 Governing Equations

The two-fluid model [4, 5] based on the theory of Khalatnicov is the most proper model to represent the thermal behaviors of superfluid helium. However, multi-dimensional analyses using original two-fluid model have been scarcely reported in the past. The reason for this is that in the momentum equation for superfluid component, the thermomechanical effect term and Gorter-Mellink mutual friction term become extremely larger than the other terms. The mathematical manipulation to solve such equations is very complex. The simplified model based on the equations for homogeneous flow has asimpler form than the original two-fluid model. Some additional terms have been added to the homogeneous flow equations to represent the heat transfer characteristics of each phase.

The simplified model consists of the following three conservation equations:

mass equation

$$\frac{\partial \rho}{\partial t}+\nabla(\rho \mathbf{u})=0 \tag{1}$$

momentum equation

$$\rho\frac{\partial \mathbf{u}}{\partial t}+(\mathbf{u}\cdot\nabla)\mathbf{u}=-\nabla p-\Delta\mathbf{M}+\mu\left[\nabla^2\mathbf{u}+\frac{1}{3}\nabla(\nabla\cdot\mathbf{u})-\Delta V\right] \tag{2}$$

energy equation

$$\rho\frac{\partial h}{\partial t}+p(\mathbf{u}\cdot\nabla)h=K \tag{3}$$

where ρ is the total density, $\mathbf{u}$ the mean velocity of total fluid, t the time, p the pressure, μ the viscosity and h the specific enthalpy. The two-dimensional forms of these equations are as follows.

mass equation

$$\frac{\partial \rho}{\partial t}+\frac{\partial(\rho u)}{\partial x}+\frac{\partial(\rho v)}{\partial z}=0 \tag{4}$$

momentum equations

$$\rho\frac{\partial u}{\partial t}+\rho u\frac{\partial u}{\partial x}+\rho v\frac{\partial v}{\partial z} \tag{5}$$

$$=-\frac{\partial p}{\partial x}-\Delta M_x+\mu\left[\left(\frac{\partial^2 u}{\partial x^2}+\frac{\partial^2 u}{\partial z^2}\right)+\frac{1}{3}\frac{\partial}{\partial x}\left(\frac{\partial u}{\partial x}+\frac{\partial v}{\partial z}\right)-\Delta V_x\right] \tag{6}$$

$$\rho\frac{\partial v}{\partial t}+\rho v\frac{\partial v}{\partial z}+\rho u\frac{\partial u}{\partial x} \tag{7}$$

$$=-\frac{\partial p}{\partial z}-\Delta M_z+\mu\left[\left(\frac{\partial^2 v}{\partial x^2}+\frac{\partial^2 v}{\partial z^2}\right)+\frac{1}{3}\frac{\partial}{\partial z}\left(\frac{\partial u}{\partial x}+\frac{\partial v}{\partial z}\right)-\Delta V_z\right]+\rho g \tag{8}$$

energy equation

$$\rho\frac{\partial h}{\partial t}+\rho u\frac{\partial h}{\partial x}+\rho v\frac{\partial h}{\partial z}=K \tag{9}$$

where u and v are the velocity in the x-direction and z-direction, respectively.

The density ρ is determined according to the state of helium.

$$\rho=\begin{cases}\rho_s+\rho_n & \text{(superfluid)}\\ \rho & \text{(normal fluid)}\\ \alpha\rho_g+(1-\alpha)\rho_l & \text{(two-phase)}\end{cases} \tag{10}$$

where α is the void fraction. The subscripts s and n indicate the superfluid component and the normal fluid component, respectively, and g and l denote the vapor phase and the liquid phase, respectively. The $\mathbf{u}$ is defined using the momentum flux of total fluid.

$$\rho\mathbf{u}=\begin{cases}\rho_s\mathbf{u}_s+\rho_n\mathbf{u}_n & \text{(superfluid)}\\ \rho\mathbf{u} & \text{(normal fluid)}\\ \alpha\rho_g\mathbf{u}_g+(1-\alpha)\rho_l\mathbf{u}_l & \text{(two-phase)}\end{cases} \tag{11}$$

$\Delta\mathbf{M}$ in Eq. (2) represents the difference between the homogeneous momentum flux and the real momentum flux. K in Eq. (3) corresponds to the heat transfer caused by internal convection in the superfluid region and heat conduction in the normal fluid region. As shown below, both $\Delta\mathbf{M}$ and K have different forms depending upon the regions.

2.2 Momentum difference

Superfluid region In the superfluid region, the real momentum flux $\mathbf{M}_{\text{real}}$ and the homogeneous momentum flux $\mathbf{M}_{\text{homogeneous}}$ can be expressed as follows:

$$\mathbf{M}_{\text{real}}=\nabla(\rho_s\mathbf{u}_s\cdot\mathbf{u}_s+\rho_n\mathbf{u}_n\cdot\mathbf{u}_n) \tag{12}$$

$$\mathbf{M}_{\text{homogeneous}}=\nabla(\rho\mathbf{u}\cdot\mathbf{u}) \tag{13}$$

Therefore,

$$\Delta\mathbf{M}=\mathbf{M}_{\text{real}}-\mathbf{M}_{\text{homogeneous}}$$

$$=\nabla(\rho_s\mathbf{u}_s\cdot\mathbf{u}_s+\rho_n\mathbf{u}_n\cdot\mathbf{u}_n)-\nabla(\rho\mathbf{u}\cdot\mathbf{u})=\nabla\frac{\rho_s\rho_n}{\rho}(\mathbf{u}_s-\mathbf{u}_n)^2 \tag{14}$$

Based on the fact that the thermomechanical effect term has almost the same magnitude as the Gorter-Mellink mutual friction term [6], it is possible to assume the following relation.

$$s\nabla T=-A_{GM}\rho_n|\mathbf{u}_s-\mathbf{u}_n|^2(\mathbf{u}_s-\mathbf{u}_n) \tag{15}$$

where A_{GM} is the Gorter-Mellink coefficient. Strictly speaking, Eq. (15) is valid only for a steady state. However, for the system studied in the present study, Eq. (15) makes a good approximation, since the relaxation time of the tmperature is considerably longer than that of the velocity of the superfluid component. From Eqs. (14) and (15), the expression of $\Delta \mathbf{M}$ in the superfluid region is

$$\Delta \mathbf{M}=\nabla\left[\frac{\rho_s\rho_n}{\rho}\left(\frac{s}{A_{GM}\rho_n|\nabla T|^2}\right)^{2/3}\times\nabla T\nabla T\right] \tag{16}$$

The two-dimensional forms of $\Delta \mathbf{M}$ are as follows.

$$\Delta \mathbf{M}_x=\frac{\partial}{\partial x}\left[N\left(\frac{\partial T}{\partial x}\right)^2\right]+\frac{\partial}{\partial z}\left[N\left(\frac{\partial T}{\partial x}\right)\left(\frac{\partial T}{\partial z}\right)\right] \tag{17}$$

$$\Delta \mathbf{M}_z=\frac{\partial}{\partial z}\left[N\left(\frac{\partial T}{\partial z}\right)^2\right]+\frac{\partial}{\partial x}\left[N\left(\frac{\partial T}{\partial x}\right)\left(\frac{\partial T}{\partial z}\right)\right] \tag{18}$$

where

$$N=\frac{\rho_s\rho_n}{\rho}\left\{\frac{s}{A_{GM}\rho_n[(\partial T/\partial x)^2+(\partial T/\partial z)^2]}\right\}^{2/3} \tag{19}$$

A_{GM} is calculated using the following relation.

$$A_{GM}=\frac{\rho_s^3 s^4 T^3}{\rho_n}F(T) \tag{20}$$

where $F(T)$ is the heat conductivity function, and is evaluated from Eq. (25) as shown later.

Normal fluid region Since the normal fluid helium behaves like a conventional singlephase fluid, $\Delta \mathbf{M}$ in this region is zero.

Two-phase flow region $\Delta \mathbf{M}$ in the two-phase flow region is zero, since the homogenous model is applied in the present study.

2.3 Heat conduction

Superfulid region The heat flux caused by the internal convection of superfluid helium $\mathbf{q}_{ic}$ can be written in the form:

$$\mathbf{q}_{ic}=-\rho_s s T(\mathbf{u}_s-\mathbf{u}_n) \tag{21}$$

Thus, K in this region is

$$K=\nabla(-\mathbf{q}_{ic}) \tag{22}$$

From Eqs. (15) and (21),

$$\mathbf{q}_{ic}=-\left[\frac{1}{F(T)|\nabla T|^2}\right]^{1/3}\nabla T \tag{23}$$

where

$$F(T)=\frac{A_{GM}\rho_n}{\rho_s^3 s^4 T^3} \tag{24}$$

Generally, the form of this function is determined from experimental data. In the present study, the following form determined using the data collected by Srinivasan et al. [7] is incorporated.

$$F(T)=\frac{A_c}{\rho^2 s_\lambda^4 T_\lambda^3}\{\tau(T)[1-\tau(T)]\}^{-3} \tag{25}$$

$$\tau(T)=\left(\frac{T+c}{T_\lambda}\right)^{5.7} \tag{26}$$

where s_λ and T_λ are 1.560 kJ/kg•K and 2.168 K, respectively. A_C and c are pressuredependent parameters. At 0.1 Mpa, $A_C=1297$m•s/kg and $c = 0.01$K.

The two-dimensional form of Eq. (22) is as follows.

$$K=\frac{\partial}{\partial x}\left(\frac{1}{F(T)}\frac{\partial T}{\partial x}\right)^{1/3}+\frac{\partial}{\partial z}\left(\frac{1}{F(T)}\frac{\partial T}{\partial z}\right)^{1/3} \tag{27}$$

Normal fluid region The heat flux caused by the heat conduction of normal fluid $\mathbf{q}_c$ can be written in the form:

$$\mathbf{q}_c=-k\nabla T \tag{28}$$

where k is the thermal conductivity. Thus, K in this region is

$$K=\nabla\cdot(-\mathbf{q}_c)=\nabla\cdot(k\nabla T) \tag{29}$$

and the two dimensional form of this equation is

$$K=\frac{\partial}{\partial x}\left(k\frac{\partial T}{\partial x}\right)+\frac{\partial}{\partial z}\left(k\frac{\partial T}{\partial z}\right) \tag{30}$$

Two-phase region The heat conduction in the two-phase region should be quite small. Thus,

$$K=0 \tag{31}$$

2.4 Phase transition or phase change between two grid nodes

In the case that the phase transition or phase change occurs between two grid nodes, the heat flux at phase interface is evaluated using the following procedures.

Phase transition Figure 1(a) illustrates the phase transition occurring between two grid nodes. At the phase interface, it is assumed that the heat flux caused by the internal convection in the superfluid region $\mathbf{q}_1$ is equal to that caused by the heat conduction in the normal fluid region $\mathbf{q}_2$. From Eqs. (23) and (28), $\mathbf{q}_1$ and $\mathbf{q}_2$. are

$$\mathbf{q}_1=-\left[\frac{1}{F(T)}\frac{\partial T}{\partial x}\bigg|_1\right]^{1/3}=-\left[\frac{1}{F(T)}\frac{T_\lambda-T_m}{b\Delta x_m}\right]^{1/3} \tag{32}$$

$$\mathbf{q}_2=-k\frac{\partial T}{\partial x}\bigg|_2=-k\frac{T_{m+1}-T_\lambda}{(1-b)\Delta x_m} \tag{33}$$

Therefore,

$$\left[\frac{1}{F(T)}\frac{T_\lambda-T_m}{b\Delta x_m}\right]^{1/3}=k\frac{T_{m+1}-T_\lambda}{(1-b)\Delta x_m} \tag{34}$$

Equation (34) is the cubic equation for b. The heat flux at the phase interface is obtained from the real root of this equation.

Phase change Figure 1(b) depicts a change from liquid normal fluid to two-phase occurring between two grid nodes. It is assumed that the temperature in the two-phase region is saturation temperature T_{sat}. The heat flux at the interface $\mathbf{q}_c$ is evaluated using heat conductivity of saturated liquid $k_{sat,l}$.

$$\mathbf{q}_c=-k_{sat,l}\frac{T_{sat}-T_m}{\Delta x_m} \tag{35}$$

If a change from two-phase to vapor occurs between two grid nodes, heat conductivity of saturated vapor $\kappa_{sat,v}$ is used to evaluate q_C.

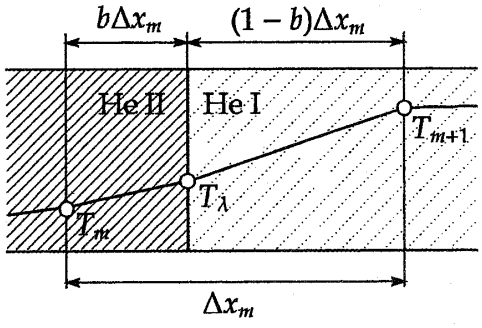

(a) Phase transition

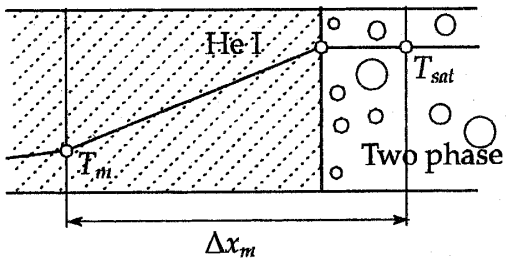

(b) Phase change

Fig. 1: Phase transition and phase change occuring between two grid nodes

$$\mathbf{q}_c = -k_{sat,v}\frac{T_{m+1}-T_{sat}}{\Delta x_m} \tag{36}$$

3 Numerical analysis

Kobayashi et al. [9] examined the temperature profiles in the horizontal channel shown in Fig. 2. The channel was initially filled with superfluid helium. The temperature in the channel was homogeneous, and it was measured as 1.95 K. The bottom of the channel was heated by locally heating section. The heat flux in the vertical direction was kept constant. The temperature in the heating section was measured using Ge thermometer, and the temperatures of helium near the bottom surface were measured using RuO_2 thermometer. Small circles in Fig. 2 indicate the positions of thermometers installed. The gaps between the thermometers and the bottom surface were fixed to 0.5 $\pm$ 0.05 mm.

In the present study, two-dimensional numerical analysis is performed on the system shown in Fig. 3. In order to avoid numerical instability at the edge of heating section, the channel length is extended but the length of the heating section is the same as the experimental system.

The finite difference method is used in the analysis. The upwind scheme of first order is applied to the convection term, while the central difference scheme of second order is employed to the other terms. Time integration is carried out implicitly using the SIMPLER method [10] with a time step of 10^{-6} sec. For numerical stability, the non-linear filter

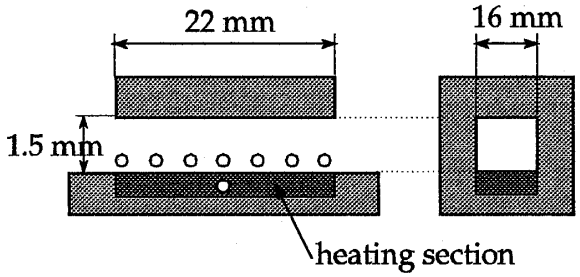

Fig. 2: Experimental system-Small circles are positions of thernometers installed.

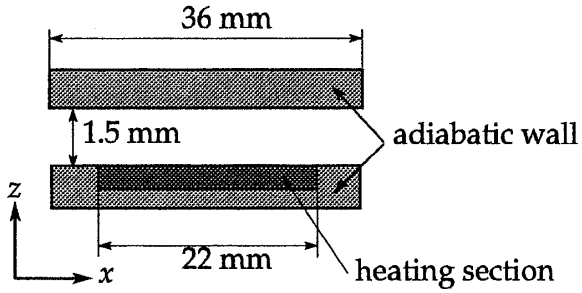

Fig. 3: Analyzed system

method [11] is used. The temperature and pressure in the channel are initially set to 1.95 K and 1 atm, respectively. The following boundary conditions are given.

- Top and bottom boundaries (except the surface of heating section):

$$\frac{\partial p}{\partial x}=0, \quad \frac{\partial T}{\partial x}=0, \quad u_x=0 \tag{37}$$

- Surface of heating section:

$$\frac{\partial T}{\partial x}=\begin{cases} F(T)q''^3 & \text{(superfluid)} \\ \dfrac{q''}{k} & \text{(normal fluid)} \\ 0 & \text{(two-phase)} \end{cases} \tag{38}$$

- Left and right boundaries:

$$p=p_0, \quad T=T_0, \quad u_x=0 \tag{39}$$

where q'' and u_x are heat flux and velocity in the x-direction, respectively.

4 Results and Discussions

4.1 Steady-state temperature profiles

The temperature profiles on a steady state obtained from the numerical analysis were compared with those from the experiment. Figure 4(a) shows the comparisons for the lower heat flux, with the fluid in the channel being kept in a superfulid state. The temperature profiles tend to be peak at the center of the channel since the heat input from the heated

section is transported to the whole fluid immediately. For the heat fluxes of 0.6, 0.639 or 0.7 W/cm², the analytical profiles show quantitative agreement with the experimental profiles. For the heat flux of 0.739 W/cm², however, the analytical profile has poor agreement with the experimental profile. The main reason for this is that in the experiment the heat transport might be partially prevented by the λ-transition occurring at the center.

Figure 4(b) shows the comparisons for higher heat flux. The λ-transition occurring at the center causes an extreme temperature increase. For the heat flux of 0.836 W/cm², an asymmetrical temperature profile appears in both the analysis and the experiment. The analysis has a slight numerical instability that can be explained as the appearance of

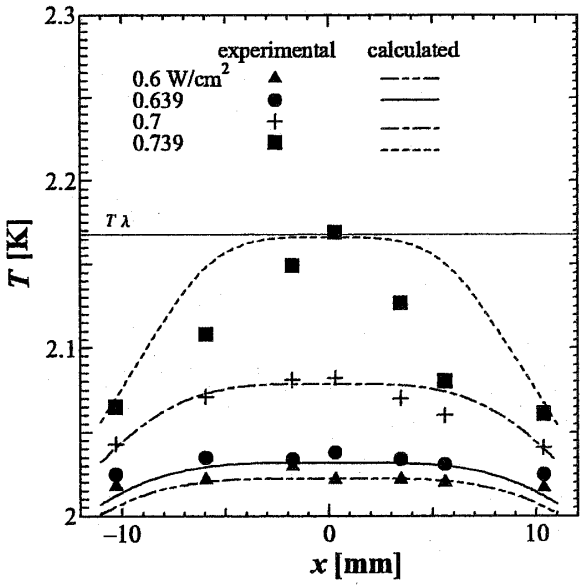

(a) lower heat flux

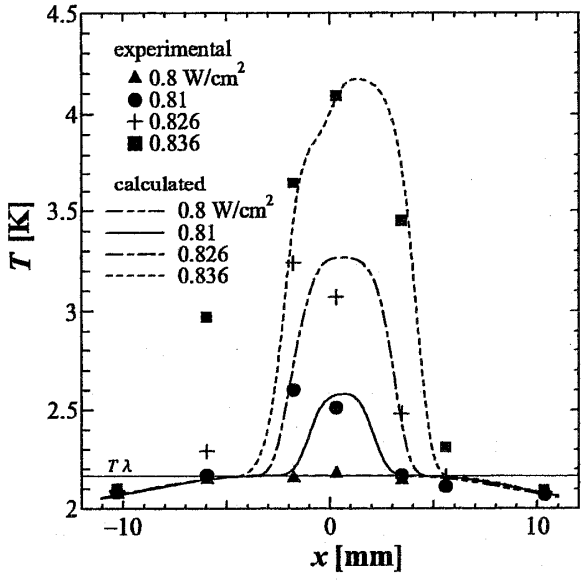

(b) higher heat flux

Fig. 4: Steady-state temperature profiles obtained from the analysis and experiment

disordered convection cells on the natural convection of normal fluid.

4.2 Trasient temperature profiles and velocity fields

Figure 5 shows temperature profiles and velocity fields obtained from the transient analysis. The heat flux is fixed to 0.81 W/cm². Each vector in the velocity fields represents the directions of velocity.

As shown in Fig. 5(a), after 0.9 sec from the start of heating, no temperature gradient in a vertical direction appears, since the whole fluid in the channel is beging kept in a superfulid helium state. The velocity vectors in the middle level have the direction from the center to the edge, while the vectors in the lower and higher level have opposite direction. This observation is due to the internal convection of superfluid components. The normal fluid components heated at the center flow to the edge, while the superfluid components flow to the center by the mass conservation. Since the normal fluid components flow faster in the

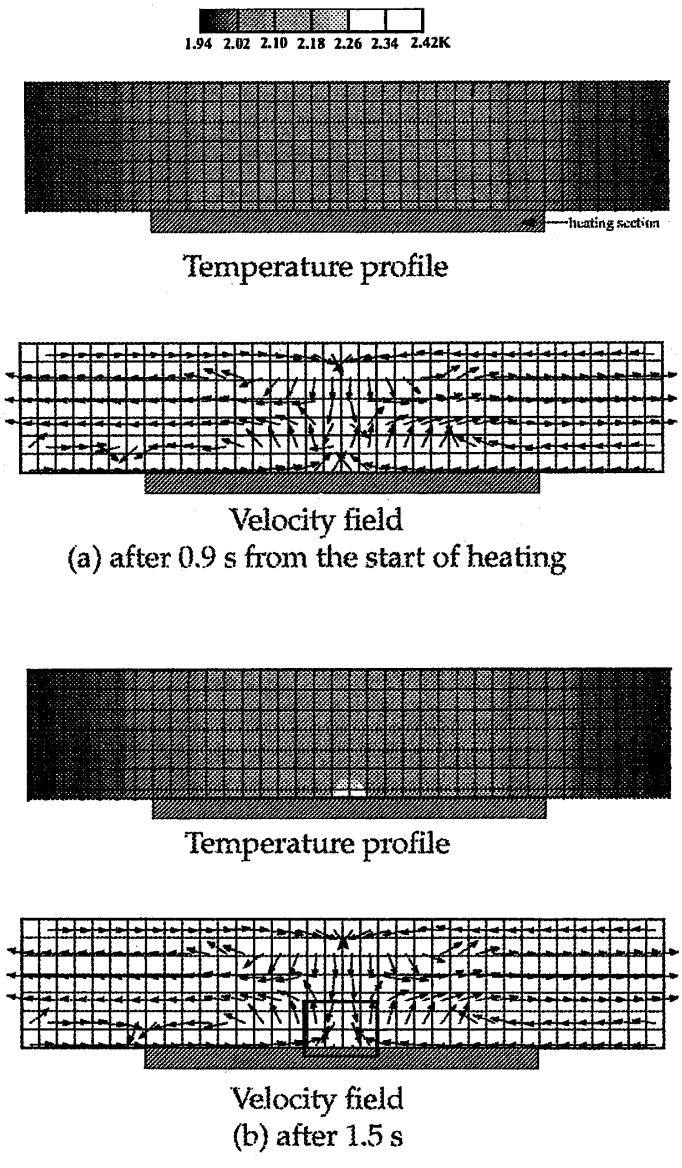

Fig. 5: Transient temperature profiles and velocity fields

middle level, the superfluid components tend to flow in the lower and higher level by Gorter-Mellink mutual friction. After 1.5 sec, as shown in Figure 5(b), a slight change in the velocity field appears since the λ-transition occurs at the center of the lower level.

5 Conclusion

A two-dimensional analysis of the horizontal channel filled with superfluid helium was performed using the numerical model proposed in the previous paper. The model is applicable to the wide temperature range from superfluid helium to normal fluid helium at vapor state. For low heat flux, the steady-state temperature profiles obtained from the analysis showed quantitative agreement with those from the experiment. For higher heat flux, the analytical results were able to simulate experimental temperature profiles reasonably well but not as accurately. The changes in velocity fields caused by the phase transition were observed in the transient analysis The validity of the proposed model in the temperature range including the phase transition was partially verified.

References

[1] Gorbounov, M. B. et al, 1996, Adv. Cryog. Eng. 41, 335.
[2] Noda, T. et al., 1998, Cryogenic Engineering, 33, 782.
[3] Noda, T. et al., 1998, Proc. of the 11th Int. Heat Trans. Conf., Kyongju, Korea, 4, 219.
[4] Tisza, L., 1938, Transport phenomena in He II, Nature, 141, 913.
[5] Landau, L., 1941, The theory of superfluidity of helium II, j. Phys. Moscow, 5, 71-90.
[6] Gorter, C. J. and Mellink, J. H., 1949, Physica, 15, 285.
[7] Srinivasan, R. and Hofmann, A., 1985, Cryogenics, 25, 652.
[8] Kashani, A. et al., 1989, Numerical Heat Transfer, Part A, 16, 213.
[9] Kobayashi, H., Osakabe, j., Tanifuji, T. and Tomita, M., 1999, Cryostatic stabilization of a large superconducting coil in pressurized superfluid helium, Applied Superconductivity, Institute of Physics Conference Series Number 167, 1, 1271-1274.
[10] Patankar, S. V., 1980, Numerical Heat Transfer and Fluid Flow, Hemisphere Publishing.
[11] Shyy, W. et al., 1992, J. Comput. Phys., 102, 49.